

A simple diffusion model showing anomalous scaling

G. Rowlands¹ and J. C. Sprott²

¹*Department of Physics, University of Warwick, Coventry CV4 7AL, England*

²*Department of Physics, University of Wisconsin, Madison, Wisconsin 53706, USA*

(Received 25 April 2008; accepted 21 July 2008; published online 13 August 2008)

A number of iterated maps and one flow, which show chaotic behavior, have been studied numerically and their time evolution expressed in terms of higher-order moments $M_m(t)$. All the cases show anomalous behavior with $M_m(t) \sim t^{g(m)}$, with $g(m) \neq \alpha m$. A simple analytic treatment is given based on an effective diffusion that is dependent on both space and time. This leads to a form for $g(m)/m = a - b/m$, which is in good agreement with numerical results. This behavior is attributed to the presence of convective motion superimposed on the background diffusion, and hence this behavior is expected in a wide variety of maps and flows. © 2008 American Institute of Physics. [DOI: 10.1063/1.2969429]

I. INTRODUCTION

It is now accepted that experimental data from a wide range of observations in the form of a time series show pseudorandom or chaotic characteristics. This behavior is often quantified in terms of the Hurst exponent. If one specifies the time series as $X(t_n)$, where n runs from 1 to N , then the Hurst exponent γ is defined by

$$M_2 \equiv \sum_{n=1}^N X^2(t_n) = DN^{2\gamma},$$

where D is a constant equal to the conventional diffusion coefficient when $\gamma = \frac{1}{2}$. An associated probability distribution function (PDF) $P(X, t)$ can then be introduced and assumed to satisfy a continuous diffusion equation

$$\frac{\partial P}{\partial t} = D \frac{\partial^2 P}{\partial X^2}.$$

However, this is only consistent if the higher moments satisfy

$$M_{2m}(N) = \sum_{n=1}^N X^{2m}(t) \propto N^m.$$

Conventional diffusion theory is a pillar upon which much of modern science is based, but there are many phenomena now known for which $\gamma \neq 1/2$. Such examples arise in fluid turbulence, plasma physics, earthquake science, biophysics, and economics (see, for example, Refs. 1 and 2). The question then is whether it is possible to describe such systems by some extension of the conventional diffusion equation. However, before considering this possibility, it is necessary to describe in more detail the typical behavior common to a wide range of such phenomena.

For example, it has been found in a range of satellite data³ that although $\gamma \neq 1/2$, the moments satisfy

$$M_m(N) = \sum_{n=1}^N |X(t_n)|^m \approx A_m N^{\gamma m}$$

for large N . (We restrict ourselves to PDFs that are symmetric in X .) This behavior is incorporated into a PDF by imposing a scaling restriction

$$P(X, t) = \frac{1}{t^\gamma} P_s(X/t^\gamma, t). \quad (1)$$

It is then natural to ask what equation P_s satisfies. If one assumes that any such equation will at most only depend on second derivatives, then one finds that to be consistent with the above scaling, P_s satisfies a general form of the Fokker-Planck equation

$$\frac{\partial P_s}{\partial s} = \frac{\partial}{\partial \xi} \left\{ [C_1 \xi + C_0(2 - 1/\gamma)\xi^{1-1/\xi}] P_s + C_0 \xi^{2-1/\gamma} \frac{\partial P_s}{\partial \xi} \right\}, \quad (2)$$

where $\xi = X/t^\gamma$, C_0 , and C_1 are constants, and $s = \ln t$. The derivation of such an equation and comparison of the solution of P_s in the asymptotic limit of $s \rightarrow \infty$ with that obtained directly from data is discussed in Ref. 3. In the limit of $\gamma = 1/2$ and $s \rightarrow \infty$, the solution for P_s reduces to a Gaussian. However, for $\gamma \neq 1/2$, the PDF shows long tails with an asymptotic behavior of the form $\xi^\alpha e^{-\beta \xi}$.

A microscopic model that leads to simple scaling is readily obtained by considering the Langevin equation equivalent to the above Fokker-Planck equation (2)

$$\frac{d\xi}{ds} = C(\xi) + \sqrt{D(\xi)} W(s),$$

where $W(s)$ symbolizes white noise, $C(\xi)$ describes convective behavior, and $D(\xi)$ represents diffusion. Here $C(\xi) = C_1 \xi + C_0(2 - 1/\gamma)\xi^{1-1/\gamma}$ and $D(\xi) = C_0 \xi^{2-1/\gamma}$. Note that, except for $\gamma = 1/2$, the presence of diffusive behavior ($C_0 \neq 0$) implies enhanced convection in both the Langevin and Fokker-Planck formulations.

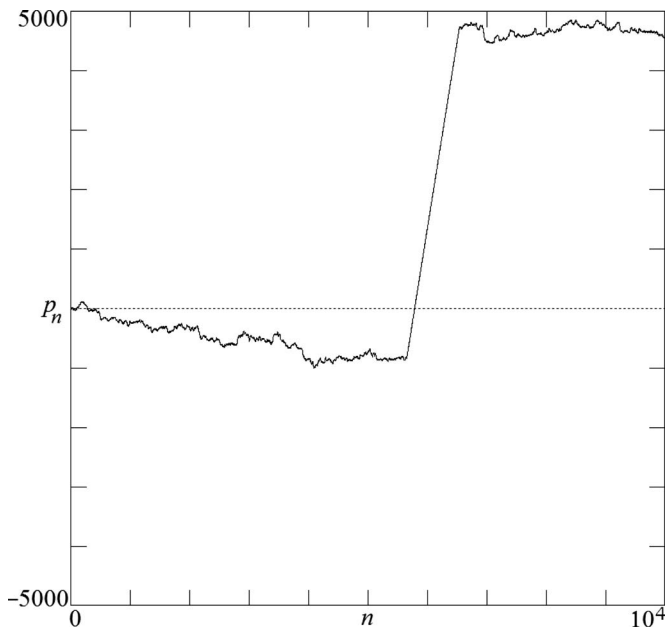


FIG. 1. Intermittency in the Chirikov map for $K=2.2\pi$.

However, not all data show the scaling described above. A classic example is fluid turbulence where the low-order moments show a more generalized scaling of the form

$$M_m(N) = A_m N^{g(m)}.$$

This is usually referred to as multiple scaling to distinguish it from the single scaling described above where $g(m) = \gamma m$. Multiple scaling is usually taken as evidence of intermittency. A detailed discussion of the implications of the above form and its relation to the turbulent flow of liquids is given by Frisch and Kolmogorov.⁴

Although the Navier–Stokes equations of fluid dynamics probably lead to multiple scaling as described by Ref. 4, the computational, analytic, or experimental effort needed to understand the relationship is huge. In the following, we discuss both numerically and analytically two maps, the Chirikov map,² the Weiss map,⁵ and a flow proposed by Thomas,⁶ show that the moments scale as above, and obtain a form for $g(m)$. Although the time series for these three examples show intermittency, the physical basis for the non-standard behavior in each case is different.

The models discussed in this paper arise naturally in plasma physics, as outlined below, and have solutions that are examples of what Shlesinger *et al.*⁷ call “strange kinetics.” That is a more or less random motion, which is diffusionlike, which itself is interrupted by large jumps that show “ballistic” behavior. An example showing this behavior in the Chirikov map is illustrated in Fig. 1, while the paper by Sprott and Chlouverakis⁸ gives an example arising in a continuous-time system. For the Chirikov map, Shlesinger *et al.*⁷ relate this ballistic motion to the presence of holes in a phase space around which the particle motion is controlled by cantori in space. This leads to the possibility of a particle getting stuck in an accelerator mode for a limited time, which leads to the ballistic motion. Their paper should be consulted for an in-depth discussion of this phenomenon. In

the Weiss map model, which describes the motion of particles in a traveling wave, the particles in the chaotic region can be trapped in nearly periodic orbits for a limited time. This stickiness is analogous to but different from the stickiness of the accelerator modes. The Labyrinth model is a continuous-time model describing Lagrangian chaos.⁹ The numerically obtained solutions suggest the presence of holes in phase space through which the particle can move freely for a limited time⁸ giving rise to ballistic motion. At present we have no detailed microscopic theory of the particle motion in or near these holes, and so we simply call them “worm holes.”

The microscopic approach as discussed in Shlesinger *et al.*⁷ leads naturally to questions such as “what is the probability of ballistic motion and what is the stickiness factor?” However, in this paper we consider a macroscopic approach by considering the structure of the moments as defined above and in particular the higher-order moments. We expect and find evidence for “ballistic” behavior in all our examples, but we do not look closely at the detailed phase space behavior.

For conventional diffusion, it is well known that the moments scale exactly as $g(m)/m = \frac{1}{2}$ and the PDF is Gaussian, that is $P(x) \sim \exp(-ax^2)$. However, for all the models considered in this paper, and for what we believe is common behavior, $g(m)/m$ is not constant and the PDF shows the presence of tails in that $P(x) \sim x$ (to some power) $\exp(-ax)$. This latter behavior is not surprising and is an indication of ballistic motion. A microscopic model, namely, that of Levy flights,¹⁰ interestingly does not show this behavior since for such cases $g(m)/m$ is a constant.

Although we consider here data generated from computer models, the approach can be easily applied to experimental data and used to study quantitatively the anomalous diffusion of plasmas in magnetic fields.

II. CHIRIKOV MAP

Introduced many years ago by Chirikov, this map has received a great deal of attention (see, for example, Lichtenberg and Lieberman²), but as far as we know, the structure of the moments, other than the second, has not been considered. The map can be written in the form

$$p_{n+1} = p_n + K \sin \theta_n,$$

$$\theta_{n+1} = \theta_n + p_{n+1},$$

where K is a constant. In the notation of the earlier section, $p_n \equiv X(t_n)$. The map is area-preserving, derivable from a Hamiltonian, and shows chaotic behavior for sufficiently large values of K . The chaos has been quantified in terms of conventional diffusion with $\gamma = \frac{1}{2}$, and the diffusion coefficient evaluated as a function of K .² However, this approach has always been treated with caution as originally pointed out by Chirikov and discussed more fully by Ishizaki *et al.*¹¹ because of the presence of so-called accelerator modes. In fact, the latter authors showed that for a range of K values, the second moment of p_n scales as a power of N but with a value of γ different from $\frac{1}{2}$. They claimed that their results

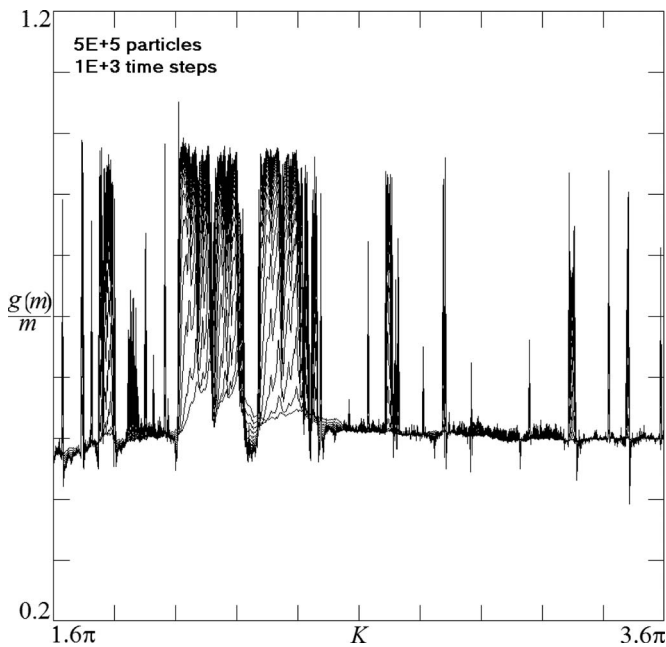


FIG. 2. Anomalous scaling in the Chirikov map as a function of K .

showed simple scaling, but they provided no evidence by calculating the higher moments.

A simple example of an accelerator mode is where the initial conditions are $p_0=0$ and $K \sin \theta_0=2\pi$. Then for all n , $p_n=2\pi n$, and $\theta_n=\theta_0 \pmod{2\pi}$. If all initial conditions behaved in a similar manner, then $M_2(N) \propto N^2$. Such solutions only occupy a small area of phase space — areas enclosed by a Kolmogorov–Arnold–Moser (KAM) surface through which trajectories cannot pass. Outside this surface is a chaotic region where trajectories can become trapped in accelerator modes but only for a finite number of iterations. It is this possibility that leads to anomalous behavior. This variation of p_n with n is illustrated in Fig. 1 where the dramatic effect of the particle becoming attached to an accelerator mode is clearly shown. There also exist higher-order accelerator modes where p increases by 2π only after several iterations, not just one. It is straightforward to illustrate this behavior by simply iterating the map for various values of K with a range of initial conditions. Care is taken to avoid initial conditions inside a KAM surface. From the generalized form of scaling introduced above, we have

$$\ln M_m(N) = g(m) \ln N + \ln A_m,$$

and hence we will refer to $g(m)$ as the slope. Since $g(m) = m/2$ corresponds to simple diffusion, we consider it as an indicator of anomalous diffusion. In Fig. 2, $g(m)/m$ is plotted versus K for values of m in the range of $1 \leq m \leq 20$. There is clear evidence of anomalous behavior for a whole range of K values. To examine the behavior more closely, three different values of K were chosen, namely, $K=2.2\pi$ where the anomalous behavior is clear, $K=3.2\pi$ where simple diffusion is expected, and $K=1.8\pi$ where the type of behavior is less clear.

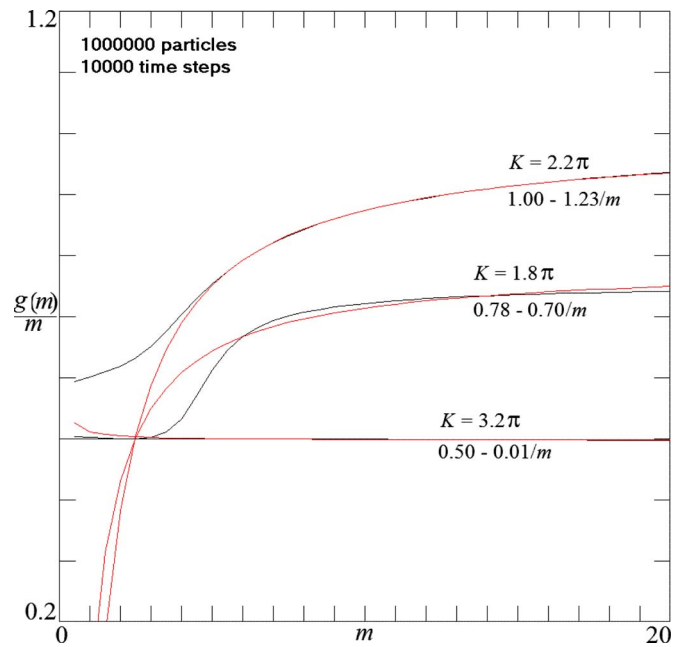


FIG. 3. (Color online) Simple and anomalous scaling in the Chirikov map as a function of m .

In Fig. 3, $g(m)/m$ is plotted as a function of m for $K=2.2\pi$ from which it is clear that since it is not constant, the behavior excludes simple scaling [$g(m)=\alpha m$]. Thus for this value of K , the map is an example of a system showing generalized scaling resulting from the strong accelerator modes.

For $K=3.2\pi$, the value of $g(m)/m$ is $\frac{1}{2}$ to within numerical error, which implies simple diffusion (constant D), consistent with the absence of an accelerator mode.

The weaker behavior for $K=1.8\pi$ in Fig. 3 is expected from the phase space plots for different K values where the number of holes associated with accelerator modes is smaller.

The variation of the PDFs with p for these three values of K is shown in Fig. 4. As expected for $K=3.2\pi$, the distribution is Gaussian, but the other two cases show the presence of long tails, the more pronounced tail being associated with $K=2.2\pi$ where the strongest accelerator modes exist.

Very similar behavior is found for a map discussed by Antonsen and Ott¹² where the p_{n+1} in the Chirikov map is replaced by $K \sin p_{n+1}$.

III. THE WEISS MAP

In a study of the effect of traveling waves on the motion of fluid particles, Weiss¹² introduced a simple map

$$x_{n+1} = x_n + k(y_{n+1}^2 - 1),$$

$$y_{n+1} = y_n - k \sin x_n.$$

Here k is a constant, which for interesting chaotic effect lies in the range $0.2 < k < 0.4$. The solution is illustrated in Fig. 5. A typical particle that starts in the chaotic channel drifts to the right with a well-defined velocity until it reaches the neighborhood of the verticals at $x=2n\pi$, where the particle

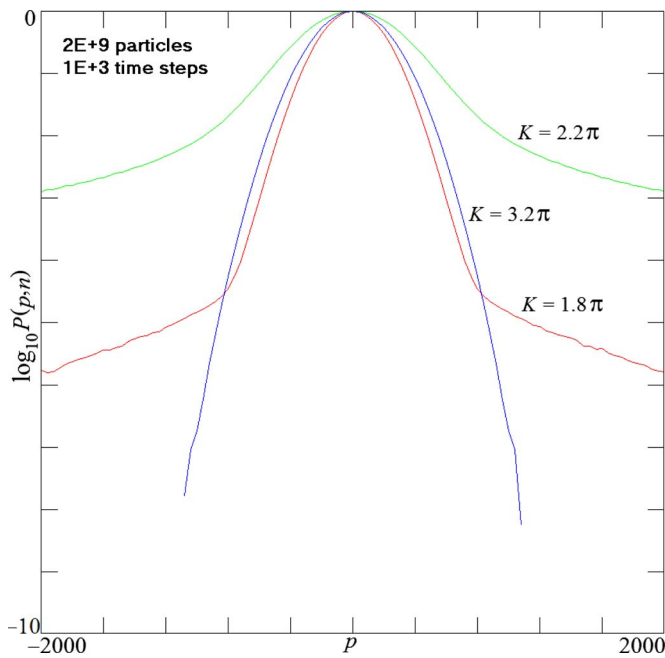


FIG. 4. (Color online) Normalized PDF for the Chirikov map after 1000 iterations.

trajectory is held up in regions of phase space. It is essentially trapped for a time as the particle goes around the broken separatrix but does not significantly change its position in x . Though no accelerator modes exist, the presence of the traveling wave produces an analogous effect. This is illustrated in Fig. 6, where the variation of $g(m)/m$ as a function of m is shown.

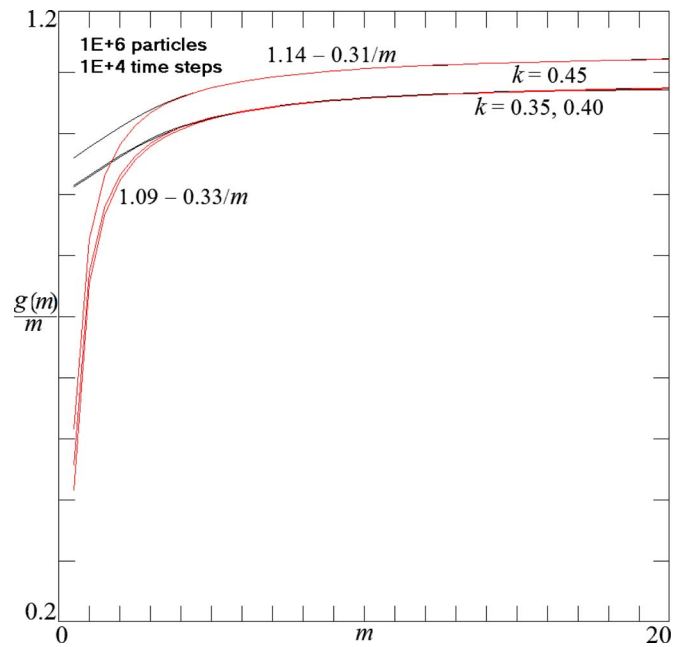


FIG. 6. (Color online) Scaling of moments in the Weiss map as a function of m .

IV. LABYRINTH MODEL

This model described by the equations

$$\dot{x} = \sin y,$$

$$\dot{y} = \sin z,$$

$$\dot{z} = \sin x,$$

was proposed by Thomas⁶ and studied in more detail by Sprott and Chlouvereakis.⁸ It shows chaotic behavior but also a form of intermittency due to the particle orbits, which normally undergo diffusive motion, but occasionally enter “worm holes”⁸ where they convectively move through phase space and then emerge later to undergo further diffusion. The approximate form of $g(m)/m$ versus m as shown in Fig. 7 fits the same pattern as for the two maps, but now the anomalous behavior is associated with the worm holes.

V. ANALYTIC TREATMENT

A simple model for studying analytically the motion of a particle when simple diffusion coexists with accelerator modes is studied in some detail by Yannaopoulos and Rowlands.¹³ In that model, a particle moves on an infinite two-dimensional lattice of points. Jumps between adjacent points mimic diffusion, while longer ones play the role of accelerator modes. In that paper, the ordinary diffusion was described in the continuum limit. Here we make a further simplification by taking the continuum limit for the accelerator modes. The results obtained in that paper show that the limiting behavior does not affect the long-time behavior of the system. Since here we are interested in the moments, and the moments themselves are only defined in the long-time limit, taking the continuum limit is justified. The basic equation is then (C6) of that paper with $N=0$. [The condition

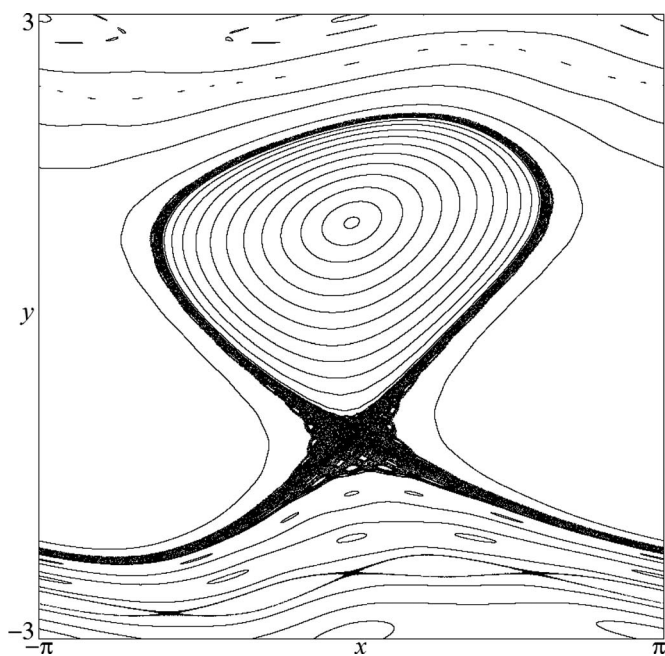


FIG. 5. The Weiss map for $k=0.4$.

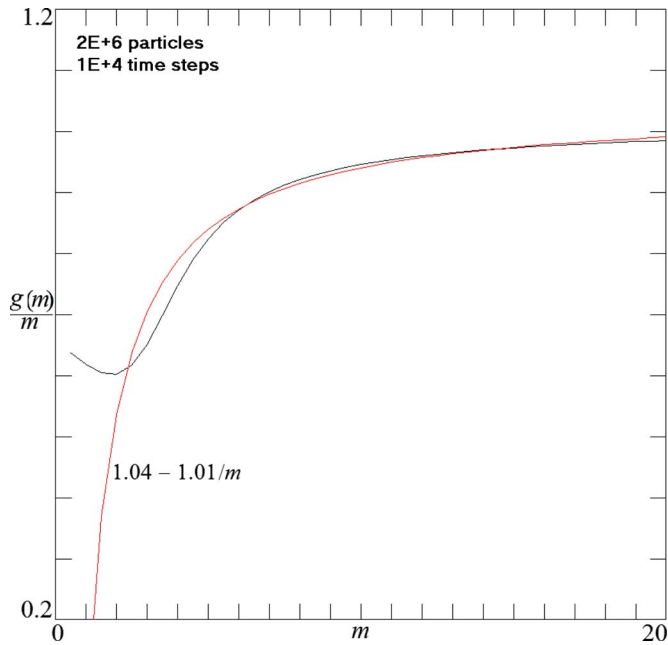


FIG. 7. (Color online) Scaling of moments in the labyrinth model as a function of m .

$N=0$ is seen to be equivalent to the continuum limit if the summation of the left-hand side of (C4) is replaced by an integral.] Then we may write this equation for the one-dimensional case in the form

$$(u + D_{\text{eff}})\hat{p}(l, u) = 1, \quad (3)$$

where

$$D_{\text{eff}} = Dl^2 - [(1 - e^{-il})\hat{\psi}(u - il) + (1 - e^{il})\hat{\psi}(u + il)].$$

Here $\hat{p}(l, u)$ is the double transform of the probability function $p(x, t)$ such that

$$p(x, t) = \int_{-\infty}^{\infty} e^{ilx} \int_0^{\infty} e^{-ut} \hat{p}(l, u) dl du.$$

Accelerator and retardor modes are included on an equal footing in the above equation, whereas (C6) only included the accelerator modes. $\hat{\psi}(u)$ is the Laplace transform of $\psi(t)$, and $\psi(t)$ is defined as the probability that a particle stays in an accelerator mode for more than a time t , divided by the time t .

In the above form, the presence of the accelerator modes gives rise to an effective diffusion D_{eff} . Given the PDF, one can calculate the even moments using the relationship

$$\hat{M}_{2p} = (-1)^p \left. \frac{\partial^{2p} \hat{p}(l, u)}{\partial l^{2p}} \right|_{l=0}.$$

However, this is only convenient for the lowest moments.

It is shown in Ref. 5 that not all forms for $\psi(t)$ lead to anomalous behavior in $M_2(t)$, but that a $\hat{\psi}(u)$ of the form $\hat{\psi}(u) = \alpha u^{\beta-1}$ corresponding to $\psi(t) \approx 1/t^\beta$ does.

For this reason, we shall assume such a form for $\hat{\psi}(u)$. Since we are interested in the large- t limit, which corre-

sponds to the small- u limit, we may expand D_{eff} as a power series in l but only retain the highest derivative of $\hat{\psi}(u)$ with respect to u . Thus

$$D_{\text{eff}} = 2 \sum_{n=1}^N (-1)^n l^{2n} \hat{\psi}^{2n-1} / (2n-1)!$$

where $\hat{\psi}^m \equiv d^m \hat{\psi}(u) / du^m$. Note that the background diffusion D does not contribute in this approximation. This sum can be expressed in closed form as

$$D_{\text{eff}} = -2l \sin\left(l \frac{d}{du}\right) \hat{\psi},$$

so that formally

$$\hat{p}(l, u) = \frac{1}{u - 2l \sin\left(l \frac{d}{du}\right) \hat{\psi}}.$$

A corresponding expansion for $\hat{p}(l, u)$ becomes increasingly complicated, and so we restrict our attention to terms up to order l^6 . This gives

$$\hat{p}(l, u) = \frac{1}{u} \left\{ 1 + \hat{\psi}' \frac{l^2}{u} + l^4 \left[\frac{4\hat{\psi}'^2}{u^2} - \frac{\hat{\psi}''}{3u} \right] + l^6 \left[\frac{\hat{\psi}'''}{60u} - \frac{4\hat{\psi}'\hat{\psi}''}{3u^2} + \frac{8\hat{\psi}'^3}{u^3} \right] + \dots \right\},$$

from which the three lowest moments are readily obtained, namely,

$$\hat{M}_2(u)/2! = (\beta - 1)\alpha u^{\beta-4},$$

$$\hat{M}_4(u)/4! = 4\alpha^2(\beta - 1)^2 u^{2\beta-7}$$

$$- \frac{\alpha}{3}(\beta - 1)(\beta - 2)(\beta - 3)u^{\beta-6},$$

$$\hat{M}_6(u)/6! = 8\alpha^3(\beta - 1)^3 u^{3\beta-10}$$

$$- \frac{4\alpha^2}{3}(\beta - 1)^2(\beta - 2)(\beta - 3)u^{2\beta-9}$$

$$+ \frac{\alpha(\beta - 1)(\beta - 2)(\beta - 3)(\beta - 4)}{60} u^{\beta-8}.$$

We are primarily interested in the dominant term in $M_m(t)$ as $t \rightarrow \infty$, which corresponds to the most singular term in $\hat{M}_n(u)$ as $u \rightarrow 0$. Then for $\beta > 1$, the above equation gives $\hat{M}_2(u) \approx u^{\beta-4}$, $\hat{M}_4(u) \approx u^{\beta-6}$, and $\hat{M}_6(u) \approx u^{\beta-8}$, suggesting a general form $\hat{M}_{2m}(u) \approx u^{\beta-2-2m}$. In the time domain, this is equivalent to $M_{2m}(t) \approx t^{2m+1-\beta}$, so that the slope $g(m)$ is given, for the even moments, by

$$g(2m) = 2m \left[1 - \frac{\beta - 1}{2m} \right].$$

It should be noted that this same form would arise if one took α as a small parameter and only retained terms proportional to α in the above expansions. Furthermore, the only

parameter that occurs in the above form for $g(m)$ is the scaling parameter β , which itself is a measure of the effectiveness of the accelerator mode to give convection.

The range of validity of this result depends on both m and β . It breaks down for small m if β is too large since then the conventional diffusion specified by the Dl^2 term must be taken into account. If this latter term dominates, then $M_2 \approx t$, so that $g(m)/m$ approaches $1/2$. In Figs. 3, 6, and 7, the function $g(m)/m$ is fitted to a function of the form $a-b/m$, with excellent agreement found for $m \geq 5$, corresponding to a value of β of order 2.

On the other hand for $\beta < 1$, the ordering of the terms in the above expression for $\hat{M}_{2m}(u)$ is different, and now the dominant behavior for $t \rightarrow \infty$ is such that $M_2(t) \approx t^{3-\beta}$, $M_4(t) \approx t^{6-2\beta}$, and $M_6(t) \approx t^{9-3\beta}$ suggesting $M_m(t) \approx t^{(3-\beta)m/2}$, so that

$$\frac{g(m)}{m} = \frac{3-\beta}{2}.$$

Thus for $\beta < 1$ the system behaves in a manner which shows the simple scaling found experimentally in satellite data.

Much of the behavior discussed above can be understood by considering the Fourier–Laplace transform of the probability density function of the Chirikov map and the simple scaling distribution discussed above. If $P(x, t)$ satisfies the scaling implied by Eq. (1), then the transformed function must satisfy Eq. (3) with $D_{\text{eff}} = l^{1/\gamma} f(l/u^\gamma)$, where f is an arbitrary function. For the Chirikov map, the approximate transformed PDF is given by Eq. (3), which for the case where $\hat{\psi}(u) = \alpha u^{\beta-1}$, is such that $D_{\text{eff}} = u + l^\beta F(l/u)$. These two expressions are similar, but as seen above, the time variation of their moments are fundamentally different.

By virtue of these two examples, we now consider the general form $D_{\text{eff}} = l^a H(l/u^b)$, where a and b are arbitrary constants and H is an arbitrary function. Then we may write

$$M_n(t) = \int P(x, t) x^n dx = \int \frac{x^n e^{ilx} e^{ut}}{u + l^a H(l/u^b)} dx du dl,$$

which with the substitutions $lx = z$, $ut = s$, and $l/u^b = q$ reduces to

$$M_n(t) = t^{bn} \int \frac{R(s, q, z)}{1 + q^{a-1} H(q)(s/t)^{ab-1}} dz ds dq,$$

where R is independent of t . Then for the case of simple scaling where $a = 1/\gamma$, $b = \gamma$, and $ab = 1$, we have $M_n(t) \propto t^{\gamma n}$. For the model of the Chirikov map, $a = \beta$, $b = 1$, and $ab - 1 = \beta - 1$. Then for $\beta > 1$, the denominator in the above integral can be expanded to give

$$M_n(t) = t^{bn} [A_1 + A_2/t^{\beta-1} + \dots].$$

However, A_1 is simply the case where $H = 0$, which is identically zero for $n > 0$, and thus $M_n(t) \approx t^{n[1-(\beta-1)/n]}$. The time variation of $M_n(t)$ agrees with that obtained by the expansion method and the numerical results for $K = 2.2\pi$.

For a general a and b such that $ab > 1$, the above discussion holds and

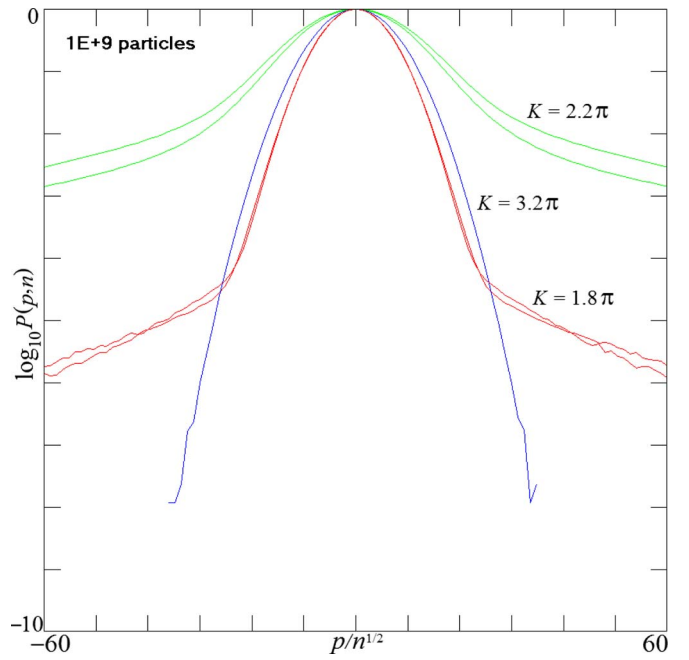


FIG. 8. (Color online) Normalized PDFs for the Chirikov map at two different times.

$$M_n(t) \approx t^{bn[1-(ab-1)/bn]}.$$

This is the form that describes the numerical results for $K = 1.8\pi$. Also note that for $ab < 1$ the unit term in the denominator can be neglected and the above generalized form for $M_n(t)$ holds.

In summary, the different types of variation with t of the n th moment can be understood in terms of the scaling of $D_{\text{eff}}(l, u)$. The discrepancies found between the analytic forms for $M_n(t)$ and the numerical results for small values of n suggest that the scaling assumption made for the form of $D(l, u)$ is not true for small l . This is as expected since for example the background diffusion has been omitted.

The PDF for the case where $D_{\text{eff}} = l^a H(l/u^b)$ takes the form

$$P(x, t) = \frac{1}{l^b} P_s(\xi, t^{ab-1}),$$

where $\xi = x/t^b$. Then by analogy with the treatment of the simple scaling case where $ab = 1$ and $b = \gamma$ and discussed in Ref. 3, we can make a reasonable approximation using the Fokker–Planck equation to describe the dynamics of $P(x, t)$. In fact, it is identical to Eq. (2) but with s replaced by $(ab-1)s$. For the case of simple scaling ($ab = 1$), this means that P_s is independent of time. However, in general we expect P_s to vary with t on a scale of $(ab-1)\ln t$. This behavior is confirmed by the simulations of the Chirikov map as shown in Fig. 8, where it is noted that the case $K = 2.2\pi$ with the larger value of $(ab-1)$ has the larger change as time advances.

Yannaopoulos and Rowlands¹⁴ have also proposed a simple model to describe the anomalous behavior found in the Weiss map. They showed in particular that the first two moments scaled such that $M_n \approx t^{n\gamma}$ for the case where the

trapping rate $\psi(t)$ scaled as t^β . However, it has not been possible to give simple analytic forms for the higher moments. Although no accelerator modes are present, the presence of an externally imposed traveling wave plays the same role.

VI. DISCUSSION

Two distinct maps, the Chirikov and Weiss maps, and a flow, the labyrinth model have been solved numerically, and the various moments $M_m(t)$ calculated as a function of time. All these cases show the same anomalous behavior in that $M_m(t)$ scales as $t^{g(m)/m}$ for large t , where $g(m)/m \approx \alpha - \beta/m$ for sufficiently large m ($m > 2$). This behavior is associated with the intermittent behavior of the “particle” motion, but the cause of intermittency is different for the three cases. For the Chirikov map it is due to the accelerator modes, for the Weiss map by the fact that the “particles” can move in the presence of a traveling wave, and for the labyrinth model by the existence of worm holes in the phase space. These three effects all have in common that they provide a convective motion superimposed on background diffusion.

The anomalous behavior in the moments is associated with the long tails that exist in the PDFs, and is illustrated in Fig. 4. For $K=3.2\pi$, which shows no anomalous behavior, the PDF is a Gaussian. For $K=1.8\pi$, which is only weakly anomalous, the tails are themselves weak, corresponding to the absence of primary accelerator modes but the presence of higher-order modes. For $K=2.2\pi$, where the primary accelerator modes are clearly present, the PDF develops pronounced tails.

All this behavior can be modeled by a generalized diffusion $D_{\text{eff}}(l, u)$ that scales such that $D_{\text{eff}}(l, u) = l^a H(l, u^b)$. The time and space evolution of the associated PDF satisfies a generalized Fokker–Planck equation, which is now nonlocal both in space and time.

For the critical case where $a=1/b$, the PDF shows the scaling commonly found in astrophysical data analyzed in Ref. 3.

From this study it is expected that if some physical mechanism exists that gives rise to convective motion in the appropriate phase space, then anomalous behavior as described in this paper is expected. This will show up in the scaling of the higher moments $M_m(t)$ and will be associated with long-tails in the PDF.

ACKNOWLEDGMENTS

This work was supported by the U.S. Department of Energy and by the National Science Foundation Center for Magnetic Self-Organization in Laboratory and Astrophysical Plasmas.

¹D. Sornette, *Critical Phenomena in Science: Chaos, Fractals, Self-Organization and Disorder* (Springer-Verlag, Berlin, 2000).

²A. J. Lichtenberg and M. A. Leiberman, *Regular and Chaotic Dynamics*, 2nd ed. (Springer, New York, 1992).

³B. Hnat, S. C. Chapman, and G. Rowlands, *Phys. Rev. E* **67**, 056404 (2003).

⁴U. Frisch and A. N. Kolmogorov, *The Legacy of Turbulence* (Cambridge University Press, Cambridge, 1995).

⁵J. B. Weiss, *Phys. Fluids A* **3**, 1379 (1991).

⁶R. Thomas, *Int. J. Bifurcation Chaos Appl. Sci. Eng.* **9**, 1889 (1999).

⁷M. F. Shlesinger, G. M. Zaslavsky, and J. Klafter, *Nature (London)* **363**, 363 (1993).

⁸J. C. Sprott and K. E. Chlouverakis, *Int. J. Bifurcation Chaos Appl. Sci. Eng.* **17**, 2097 (2007).

⁹T. Bohr, M. H. Jensen, G. Paladin, and A. Vulpiani, *Dynamical Systems Approach to Turbulence* (Cambridge University Press, Cambridge, 1998).

¹⁰E. W. Montroll and M. F. Schlesinger, in *Non Equilibrium Phenomena II from Stochastics to Hydrodynamics*, edited by J. L. Lebowitz and E. W. Montroll (Elsevier, Amsterdam, 1984), pp. 1–121.

¹¹R. Ishizaki, T. Horita, T. Kobayashi, and H. Mori, *Prog. Theor. Phys.* **85**, 1013 (1991).

¹²T. M. Antonsen and E. Ott, *Phys. Fluids* **24**, 1635 (1981).

¹³A. N. Yannaopoulos and G. Rowlands, *J. Phys. A* **26**, 6231 (1993).

¹⁴A. N. Yannaopoulos and G. Rowlands, *Physica D* **76**, 216 (1994).